

**Re: Ms. Ref. No.: essd-2023-283**

We would like to express our sincere thanks for the valuable comments and constructive suggestions from the reviewers that greatly improve the quality of this manuscript (essd-2023-283: Monsoon Asia Rice calendar: a gridded rice calendar in monsoon Asia based on Sentinel-1 and Sentinel-2 images). We have made all the requested changes to the manuscript and indicated the disposition how we have incorporated the requested changes from the reviewers into the revised manuscript, which is also attached. We hope that the revised manuscript now addresses your concerns.

**Response to the anonymous reviewer's comments**

*Anonymous referee #1:*

*Zhao et al. mapped a new (2019 to 2020) gridded ( $0.5^\circ \times 0.5^\circ$  resolution) rice calendar for monsoon Asia based on Sentinel-1 and Sentinel-2 satellite images for monitoring the rice transplanting date, harvest date, and number of rice croppings. Its result may reveal the rice phenological dates for three croppings in monsoon Asia. However, three major points needed to be improved.*

We greatly appreciate the valuable and constructive comments provided by the reviewer. In the following responses, we will address each comment point-by-point. The responses to the comments are presented in blue font, and changes to the manuscript are highlighted in red with a grey background.

*#1 The authors use two steps to map the rice calendar: (1) detection of rice phenological dates and number of rice croppings through combination of a feature-based algorithm and the fitted Weibull function, and (2) spatio-temporal integration of the detected*

*transplanting and harvest dates using von Mises maximum likelihood estimates. However, there is no logical relationship between the two steps. In its current version, it seems that the authors use two different methods (combination of a feature-based algorithm and the fitted Weibull function, and von Mises maximum likelihood estimates) to monitor the rice phenological dates, but did not compare the advantages and disadvantages of the two methods. Maybe the output from step one would be the input to step two? The authors should explain the logical relationship, because this is the key of this study.*

**Response:** We extend our sincere appreciation to the reviewer for the valuable feedback. As you rightly pointed out, the output from step one would serve as the input for step two. In Step 1, we utilized a feature-based algorithm to extract the transplanting and harvest date (as detailed described in Lines 201-234 of revised manuscript). To identify the number of rice croppings, a fitted Weibull function was employed (as detailed described in Lines 235-259 of revised manuscript). Upon completing Step 1, we successfully detected all the transplanting and harvest dates across two years for each grid. However, it is important to note that these detected transplanting and harvest dates within each grid can vary annually due to different weather conditions, the impact of climate change, adjustments in agricultural schedules, and the availability of satellite images. Furthermore, the transplanting and harvest dates for a specific cropping season in one grid can significantly differ from those in neighboring grids, possibly indicating detection errors. Therefore, the spatio-temporal integration of these detected transplanting and harvest dates, referred to as Step 2, is a necessary process for generating a multi-year spatially averaged rice calendar. In response to your suggestion, we have revised the 2.3.2 Section to emphasize the key points that Step 1 is the input of Step 2. The revised contents are as follows:

- All the transplanting and harvest dates across two years for each grid were detected in Step 1 by using the algorithms and processes described above. However, these detected transplanting and harvest dates in each grid vary annually due to different

weather conditions, the effects of climate change, adjustments in agricultural schedule, and the availability of satellite images. Additionally, the detected transplanting and harvest dates for a specific cropping season in a grid can differ markedly from those in neighboring grids, possibly indicating detection errors. Therefore, the temporal and spatial integration of the detected transplanting and harvest dates, referred to as Step 2, is a necessary step for generation of a multi-year, spatially averaged rice calendar (Lines 270-276).

We have made a revision that makes the logical relationship between Step 1 and Step 2 more clear in the Abstract:

- The methodological framework incorporates two steps: (1) detection of rice phenological dates and number of rice croppings through combination of a feature-based algorithm and the fitted Weibull function, and (2) spatio-temporal integration of the detected transplanting and harvest dates derived from step 1 using von Mises maximum likelihood estimates (Lines 18-21).

At the same time, we have added arrows in Figure 2 to show that the transplanting and harvest dates obtained in Step 1 are the inputs for Step 2. Correspondingly, its description and caption have also been revised as follows:

- The overall methodology for rice calendar mapping, which is summarized in Fig. 2, can be divided into two steps. The first step is extraction of transplanting and harvest dates and detection of the number of rice croppings, depicted in Fig. 2 Step 1.-1 as the algorithm for phenological dates and number of rice croppings detection and in Fig. 2 Step 1-2 as the process of phenological dates and number of rice croppings detection. The transplanting and harvest dates obtained in the first step

(Step 1) require temporal and spatial integration for the generation of the rice calendar (Fig. 2 Step 2) (Lines 188-192).

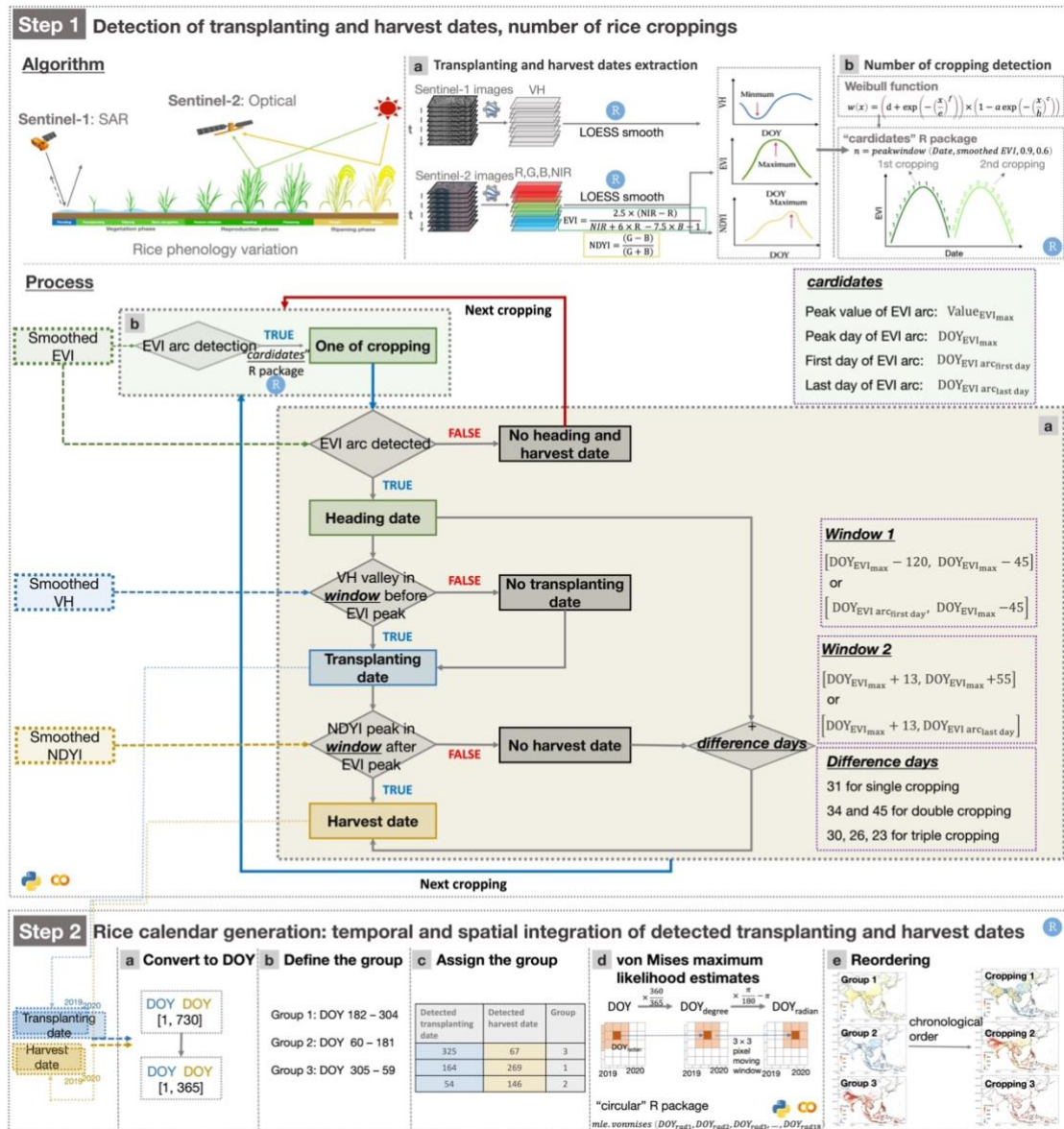


**Figure 2.** Workflow for gridded rice calendar mapping based on satellite images. Step 1 depicts the algorithm and process of transplanting and harvest dates extraction, along with the detection of number of rice croppings, as shown in the first box. In Step 2, the generation of the rice calendar is described, relying on the detected transplanting and harvest dates derived from Step 1, through the temporal and spatial integration of the detected phenological dates displayed in the second box (Page 9).

Moreover, we have improved the paragraph that emphasizes the derivation of Step 2 from Step 1 in the Results and Discussion section:

- Temporal and spatial integration of detected transplanting and harvest dates, as derived from Step 1, pose a great challenge owing to flexible agricultural schedules, and the availability of satellite imagery (Lines 489-490).

*#2 The validation of the accuracy of the results is weak and scarce. The authors only compare the identified rice phenological dates with the existing products, including the RiceAtlas rice calendar, the RICA rice calendar, and the SAGE rice calendar, instead of field observation of rice phenology. It is inappropriate because the existing products themselves have identification errors, thus lacking of reliability. Therefore, it is meaningless to verify the detection results using the biased information. The authors should add the contents about verifying the results with actual field observations of rice phenology.*

**Response:** We sincerely thank the reviewer for the valuable comment. We acknowledge the critical role of rice calendar accuracy in validating the precision of our proposed rice calendar. We completely understand the review's concerns about the accuracy of existing rice calendars, which may contain the uncertainties due to several reasons. It is worth noting that we have addressed this issue in detail in the "3.4 Uncertainty" as follows:

- The accuracy of reference rice calendars should also be considered, as they may rely on data from various sources and administrative scales (Laborte et al., 2017). Overlapping phenological dates between rice cropping seasons (Figs. S6-S8) can introduce further uncertainty (Lines 524-526).

Regarding RiceAtlas, despite the presence of detection errors, it remains the only detailed global rice calendar to date (Laborte et al., 2017). Since its publication in 2017,

RiceAtlas rice calendar has been cited 84 times (according to Web of Science). It stands as the widely accepted rice calendar extensively used in numerous research domains, including rice calendar validation (e.g., RICA rice calendar in Mishra et al. (2021), Iizumi et al. (2019)), mapping rice paddy field distribution (Han et al., 2021; Luintel et al., 2021), predicting rice production (Oort et al., 2017; Wu et al., 2023), and estimating methane emissions (Crippa et al., 2020; Ouyang et al., 2023). In fact, researchers regard RiceAtlas as the standard database for comparing rice phenology based on earth observation (Mishra et al., 2021).

Our primary objective here is to compare the differences among similar large-scale rice calendar products. The improved accuracy of our proposed rice calendar, which outperformed the RICA rice calendar when compared with RiceAtlas rice calendar, highlights the critical importance and necessity of our proposed rice calendar. Our proposed rice calendar can integrate the strengths, such as consistent detection through remote sensing methods as seen in the RICA rice calendar, while addressing the weaknesses, such as the coarse spatial resolution found in existing large-scale rice calendars like RiceAtlas and RICA rice calendars and limited number of rice cropping seasons in the SAGE rice calendar). This effort has resulted in the development of our new, spatially explicit rice calendar.

As reviewer rightly point out, actual field observations are essential for validating the accuracy of rice phenology detection methods. Fortunately, we have previously validated the rice phenology detection methods (feature-based algorithm) used in this rice calendar production in a prior study using actual field observations (Zhao et al., 2023). Results revealed a bias of 4 and -13 days for transplanting and harvest dates, respectively (as shown in Fig. 6, Fig. 7, Table 1, and Appendix A in Zhao et al. (2023)). Moreover, we employed various spatial scales, including actual site observations, sub-national, and 0.5° gridcell scales, to rigorously validate our feature-based algorithm, ensuring its robustness (Zhao et al., 2023). We have added this description in the revised manuscript as follows:

- A feature-based algorithm, proposed for large-scale rice phenology detection (Zhao et al., 2023), excels in utilizing backscattering (VH) and vegetation indices (Enhanced Vegetation Index (EVI) and Normalized Yellow Index (NDYI)) derived from Sentinel-1 & 2 to reflect features related to rice cultivation such as flooding, maximum leaf area, and most yellowness around transplanting, heading, and harvest date. Additionally, this algorithm has successfully tracked rice phenological dates in different cropping systems (single, double, and triple croppings) and at different spatial scales (sub-nation, 0.5° gridcell, and site scales) (Zhao et al., 2023) (Lines 94-99).
- These phenological characteristics of rice crops can be captured by a feature-based algorithm applied on smoothed VH, EVI, and NDYI time series data (Zhao et al., 2023). This algorithm's robustness has been confirmed at multiple spatial scales (sub-nation, 0.5° gridcell, and site scales) and cropping systems (single, double, and triple croppings) in monsoon Asia (Zhao et al., 2023). The transplanting date was determined by identifying the minimum VH intensity from the shortest plants above the water surface, where VH intensity gradually increase as they interact with the radar signal (Torres et al., 2012). The harvest date was detected using the NDYI's yellow signal, indicating the maximum yellowness at harvest date (Zhao et al., 2023) (Fig. 2 Step 1 Algorithm a) (Lines 210-221).

In summary, our proposed rice calendar has undergone validation using other rice calendar products as well as through field observations of rice phenology. We hope this addresses your concerns adequately.

## References

Zhao, X., Nishina, K., Akitsu, T.K., Jiang, L., Masutomi, Y., Nasahara, K.N.: Feature-based algorithm for large-scale rice phenology detection based on satellite images, *Agric. For. Meteorol.*, 329, 109283, <https://doi.org/10.1016/j.agrformet.2022.109283>, 2023.

Laborte, A.G., Gutierrez, M.A., Balanza, J.G., Saito, K., Zwart, S.J., Boschetti, M., Murty, M.V.R., Villano, L., Aunario, J.K., Reinke, R., Koo, J., Hijmans, R.J., and Nelson, A.: RiceAtlas, a spatial database of global rice calendars and production, *Sci. Data*, 4, 170074, <https://doi.org/10.1038/sdata.2017.74>, 2017.

Mishra, B., Busetto, L., Boschetti, M., Laborte, A., Nelson, A.: RICA: A rice crop calendar for Asia based on MODIS multi year data. *Int. J. Appl. Earth Obs. Geoinf.* 103, 102471, <https://doi.org/10.1016/j.jag.2021.102471>, 2021.

Iizumi, T., Kim, W., and Nishimori, M.: Modeling the global sowing and harvesting windows of major crops around the year 2000. *J. Adv. Model. Earth Syst.*, 11(1), 99-112, <https://doi.org/10.1029/2018MS001477>, 2019.

Han, J., Zhang, Z., Luo, Y., Cao, J., Zhang, L., Cheng, F., Zhuang, H., Zhang, J., Tao, F.: NESEA-Rice10: high-resolution annual paddy rice maps for Northeast and Southeast Asia from 2017 to 2019. *Earth Syst. Sci. Data*, 13, 5969-5986, <https://doi.org/10.5194/essd-13-5969-2021>, 2021.

Luintel, N., Ma, W., Ma, Y., Wang, B., Xu, J., Dawadi, B., Mishra, B.: Tracking the dynamics of paddy rice cultivation practice through MODIS time series and PhenoRice algorithm. *Agric. For. Meteorol.*, 307, 108538, <https://doi.org/10.1016/j.agrformet.2021.108538>, 2021.

van Oort, P.A.J. and Zwart, S.J.: Impacts of climate change on rice production in Africa and causes of simulated yield changes. *Glob. Change Biol.*, 24, 1029-1045, <https://doi.org/10.1111/gcb.13967>, 2018.

Wu, H., Zhang, J., Zhang, Z., Han, J., Cao, J., Zhang, L., Luo, Y., Mei, Q., Xu, J., Tao, F.: AsiaRiceYield4km: seasonal rice yield in Asia from 1995 to 2015. *Earth Syst. Sci. Data*, 15, 791-803, <https://doi.org/10.5194/essd-15-791-2023>, 2023.

Crippa, M., Solazzo, E., Huang, G., Guizzardi, D., Koffi, E., Muntean, M., Schieberle, C., Friedrich, R., Janssens-Maenhout, G.: High resolution temporal profiles in the emissions database for global atmospheric research. *Sci. Data*, 7, 121, <https://doi.org/10.1038/s41597-020-0462-2>, 2020.

Ouyang, Z., Jackson, R.B., McNicol, G., Fluet-Chouinard, E., Runkle, B.R.K., Papale, D., Knox, S.H., Cooley, S., Delwiche, K.B., Feron, S., Irvin, J.A., Malhotra, A., Muddasir, M., Sabbatini, S., Alberto, M.C.R., Cescatti, A., Chen, C., Dong, J., Fong, B.N., Guo, H., Hao, L., Iwata, H., Jia, Q., Ju, W., Kang, M., Li, H., Kim, J., Reba, M.L., Nayak, A.K., Roberti, D.R., Ryu, Y., Swain, C.K., Tsuang, B., Xiao, X., Yuan, W., Zhang, G., Zhang, Y., Paddy rice methane emissions across Monsoon Asia. *Remote Sens. Environ.*, 194, 348-365, 284, 113335, <https://doi.org/10.1016/j.rse.2022.113335>, 2023.



*#3 The authors emphasize for many times that the proposed rice calendar fills the gaps in high resolution rice calendars, like Line 27, and Line 96 (high spatial resolution, 0.5°). However, there are currently so many high resolution satellites images, like Landsat images for 30 m and Sentinel-1/2 satellite images for 10 m. The spatial resolution for 0.5° of the proposed rice calendar cannot be called high resolution.*

**Response:** We appreciate the constructive feedback provided by the reviewer and have incorporated this suggestion into revised manuscript. As you noted, it is indeed true that our proposed rice calendar, with a spatial resolution of 0.5°, may not be categorized as “high resolution” when compared to the 30 m or even 10 m high-resolution satellite images. It is also important to convey the advantage of our proposed rice calendar – our spatial resolution surpasses that of existing large-scale rice calendars, which are typically produced at administrative scale ranging from country to sub-country levels. Taking into account these two key aspects, we have refrained from using the term “high spatial resolution (0.5°)” and have also decided to quit using “finer-resolution rice calendar” in the revised manuscript.

The revised contents are specifically as follows:

- This novel gridded rice calendar fills the gaps in half-degree rice calendars across major global rice production areas, facilitating research on rice phenology that is relevant to the climate change (Lines 27-29).
- The objective of this study was to develop a new gridded rice calendar that highlights the following features: (a) consistent detection using remote-sensing methods, (b) spatial resolution (0.5° × 0.5°), (c) large-scale coverage (monsoon Asia), and (d) ability to extract multiple rice croppings (Lines 110-112).
- The advantages of the above-mentioned algorithms (Fig 2 Step 1, Step 2) largely contribute to the production of a gridded rice calendar. The proposed rice calendar

fills the gaps in finer scale rice calendars with continental coverage using remote sensing methods. The proposed rice calendar provides spatially explicit rice phenology with continental coverage through remote sensing methods. The major difference between the proposed rice calendar and the RICA rice calendar lies in the use of a feature-based algorithm with VH and NDYI, which allows the proposed rice calendar to theoretically estimate rice phenology more accurately. Zhao et al. (2023) demonstrated that VH can accurately capture the start of paddy water logging, and NDYI is a good indicator of rice maturity stage. The proposed rice calendar presents a highly patchy map of rice phenological information (Figs. 6 and 10a). The 0.5° resolution of the proposed rice calendar is finer than that of other rice calendars, including RiceAtlas, RICA at sub-national scale, and SAGE derived from sub-national data. This improvement greatly reduces the bias error caused by assigning averaged rice phenology to administrative units, as rice phenology can vary considerably within large administrative units (Franch et al., 2022). Furthermore, the proposed rice calendar displays the detailed distribution of rice paddy fields (Figs. 6 and 10a), in contrast to previous rice calendars that covered entire administrative areas, irrespective of the small proportion of rice cultivation (Figs. S6-S8 and 10b-d) (Lines 501-513).

- Given the absence of an updated global/continental-scale rice calendar that can explicitly depict spatial gridded transplanting date and harvest date information, and the number of rice croppings, this study developed a new gridded rice calendar for monsoon Asia with spatially explicit detail of rice phenology using a new methodological framework based on Sentinel-1 and Sentinel-2 images (Lines 586-589).

#### *Minor issues*

1. Line 129-130, the authors aggregated rice distribution map at 500 m resolution into 0.5° resolution by randomly selecting 20 rice fields to derive the average phenology.

*This process is unreasonable because 20 fields are not representative. It is suggested that the authors should first calculate the planting fraction for rice paddy at 0.5° resolution based on rice distribution map at 500 m resolution, derive the pixels which have a higher planting proportion like 80%, and then extracting the average phenology of above pixels.*

**Response:** We greatly appreciate the reviewer’s constructive comments. Our apologies for the ambiguous description in the previous version. The rice paddy field distribution map was aggregated to a gridded map with 0.5° resolution, INSTEAD OF converting the rice paddy field distribution map at 500 m resolution into 0.5° resolution by randomly selecting 20 rice fields to derive the average phenology. To avoid ambiguity, we have moved the sentence “This rice paddy field distribution map was aggregated to a gridded map with 0.5° resolution (Fig. 1b).” (originally located at the beginning of the sampling method paragraph) to the end of the paragraph describing the rice paddy field distribution map.

- The rice paddy field distribution map adopted in this study is from a 500 m resolution map produced using MODIS images (Zhang et al., 2020) (Fig. 1a). This map effectively displays the presence and distribution of rice paddy fields over monsoon Asia. The reliability of this map is substantiated by its strong correlation with existing rice paddy field maps across diverse areas ( $R^2$  values ranging from 0.72 to 0.95) and its alignment with the area information obtained from FAOSTAT statistical data for each country (Zhang et al., 2021). Furthermore, this map aligns well with the area information obtained from FAOSTAT statistical data for each country (Zhang et al., 2020). Additionally, this map has been used to develop a feature-based algorithm for rice phenology detection (Zhao et al., 2023). In this study, this rice paddy field distribution map was aggregated into a gridded map with 0.5° resolution (Fig. 1b).

~~This rice paddy field distribution map was aggregated to a gridded map with 0.5° resolution (Fig. 1b). Within each 0.5° grid, 20 rice paddy fields were randomly selected to derive the average rice phenology for that grid (Xiao et al., 2021; Zhao et al., 2023). This sampling method effectively minimizes errors caused by misclassification of rice paddy fields by excluding outliers that deviate from the averaged rice phenology (Zhao et al., 2023) (Lines 137-150).~~

In fact, we have already calculated the fraction of rice paddy fields at 0.5° resolution based on the rice distribution map at 500 m resolution in our research. Fig. 1b displays the percentage of rice paddy field in 0.5° grids. Green gradient indicates variation in the percentage coverage of rice paddy fields (Page 5).

From the provided fraction of the rice paddy field map (Fig. 1b), areas with a high proportion of rice cultivation are mainly located in the Indo-Gangetic Plain, the Yangtze Plain, the Ayeyarwady Delta region, and the Mekong Basin. If we extract the average phenology from these high proportion grids, we will miss the rice phenology in other grids across monsoon Asia. However, the objective of our research is to develop a gridded rice calendar that considers each grid individually. Indeed, the high proportion of rice paddy areas improves the accuracy of averaged rice phenology detection by enabling more precise identification of rice paddy fields. In contrast, our sampling method – randomly selecting 20 rice paddy fields – is suitable for both high and low proportion rice paddy area grids. It effectively selects the rice paddy fields, saving computation time and facilitates the implementation, while reducing the error of misclassification of rice paddy fields by excluding outliers that deviate from the averaged rice phenology (Fig. S2 in Supplementary in Zhao et al., 2023). The average rice phenology for each grid was therefore determined by the rice phenology that predominates in that grid.

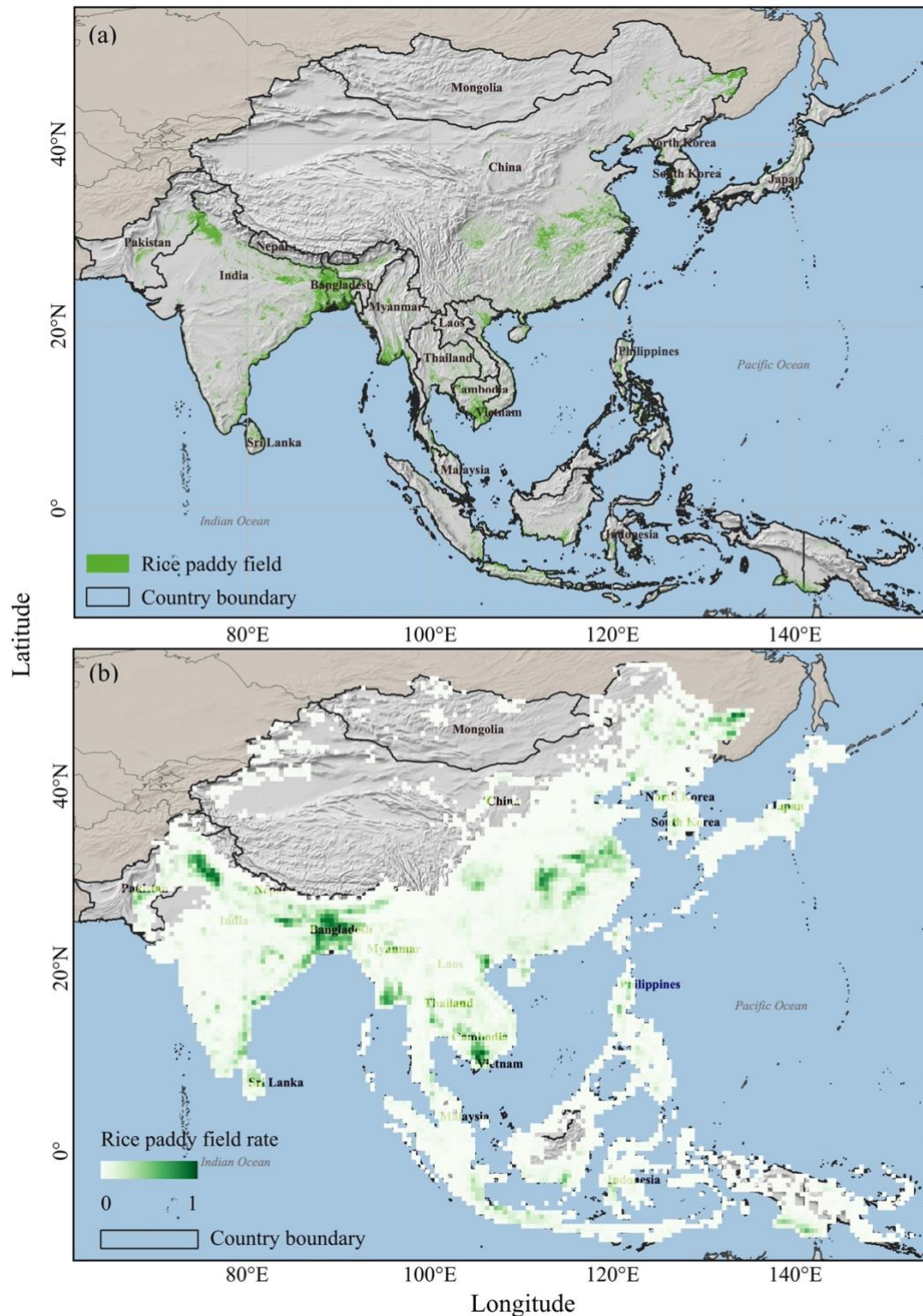


**Figure 1.** Location of the study area and distribution of rice paddy fields in monsoon Asia. Rice paddy field distribution map (a) was obtained from Zhang et al. (2020), which was produced using MODIS images. Green areas indicate rice paddy fields, and bold black borders indicate the countries in this study area. Gridded rice paddy field map (b) shows the percentage of rice paddy field in 0.5° grids. Green gradient indicates variation in the percentage coverage of rice paddy fields (Page 5).

Moreover, to demonstrate the rationale for sampling 20 rice paddy fields, we provide an example to address this issue, as shown in the following figure. In this example, 10, 20, 30, 40, and 50 rice paddy fields were randomly selected within four neighboring  $0.5^\circ$  grids. There is no difference in the extracted EVI peak days among the 20, 30, 40, and 50 sampled rice paddy fields for four grids. However, the 10 sampled rice paddy fields tend to yield different peak EVI days. We have included this figure as Fig. S2 in the Supplementary.

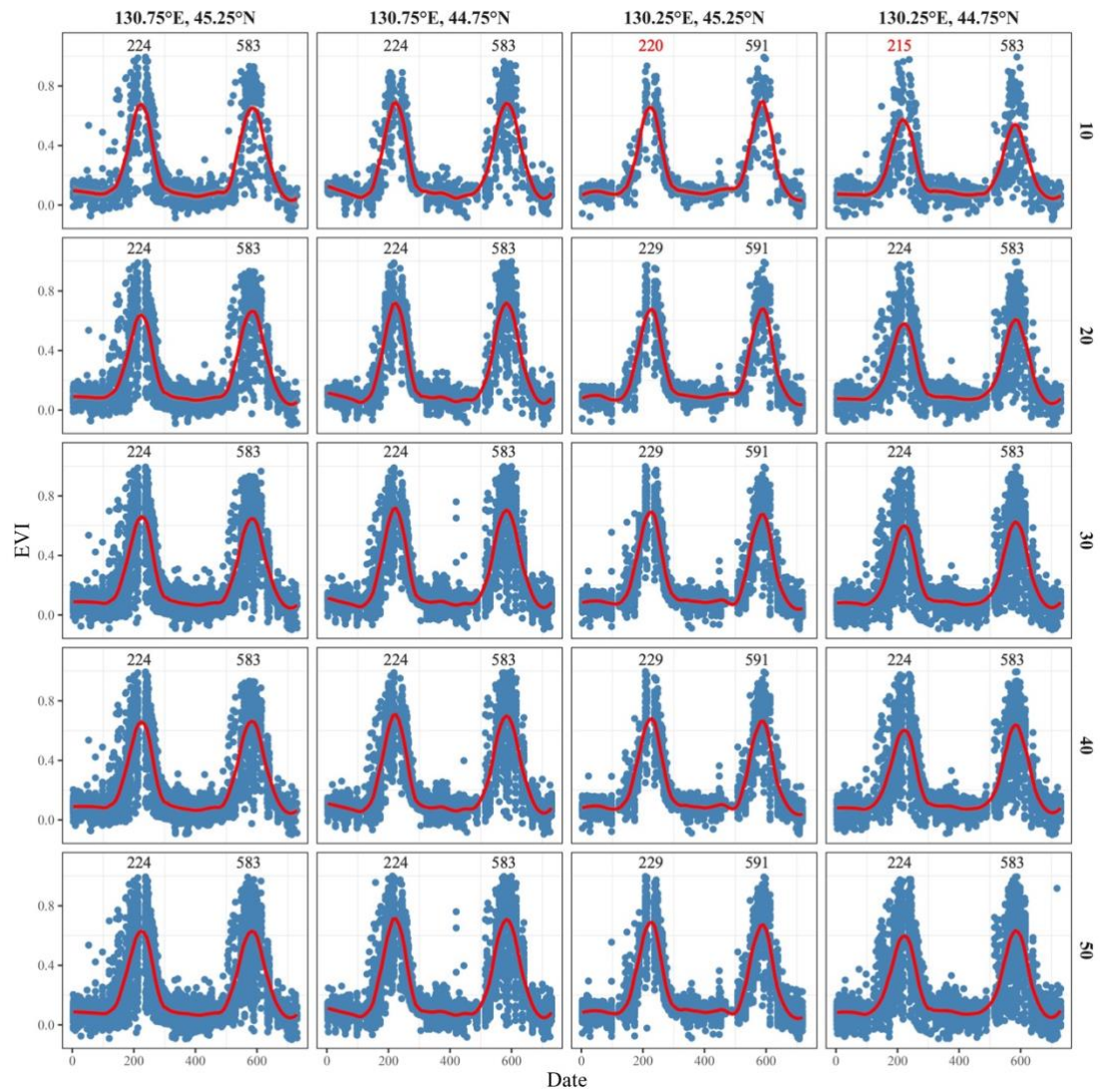


**Figure S2.** Example of the effect of sampling numbers in rice paddy fields (10, 20, 30, 40, and 50) for extracting phenological dates. X-axis denotes the days from 1 January 2019 to 31 December 2020, and Y-axis denotes the EVI

values. The red line denotes the smoothed EVI values. The number in each panel denotes the extracted peak EVI days.

We have cited Fig. S2 in the “Rice paddy field distribution map and sampling method” section to show how the sample size was determined, as follows:

➤ Additionally, this sampling size of 20 rice paddy fields is sufficiently enough that saves computation time and has no effect on averaged rice phenology detection (Fig. S2) (Lines 150-151).

2. Line 175-178, Step 1-1 and Step 1-2 describe the same thing. It is suggested that these two steps be combined.

**Response:** We greatly appreciate the reviewer’s suggestion. As you suggested, Step 1-1 and Step 1-2 depict the algorithms and processes for detecting rice phenological dates and number of rice croppings, respectively. Both of these sub-steps focus on the same issue: how to detect phenological dates and the number of rice croppings. Therefore, we have combined Step 1-1 and Step 1-2 into a comprehensive step, summarizing these two sub-steps as “Step 1 Detection of transplanting and harvest dates, number of rice croppings”. Additionally, we have revised Figure 2 and its description to correspond to this combination.

➤ The overall methodology for rice calendar mapping, which is summarized in Fig. 2, can be divided into two steps. The first step is extraction of transplanting and harvest dates and detection of the number of rice croppings, depicted in Fig. 2 Step 1.-1 as the algorithm for phenological dates and number of rice croppings detection and in Fig. 2 Step 1-2 as the process of phenological dates and number of rice croppings detection. The transplanting and harvest dates obtained in the first step (Step 1) require temporal and spatial integration for the generation of the rice calendar (Fig. 2 Step 2) (Lines 188-192).

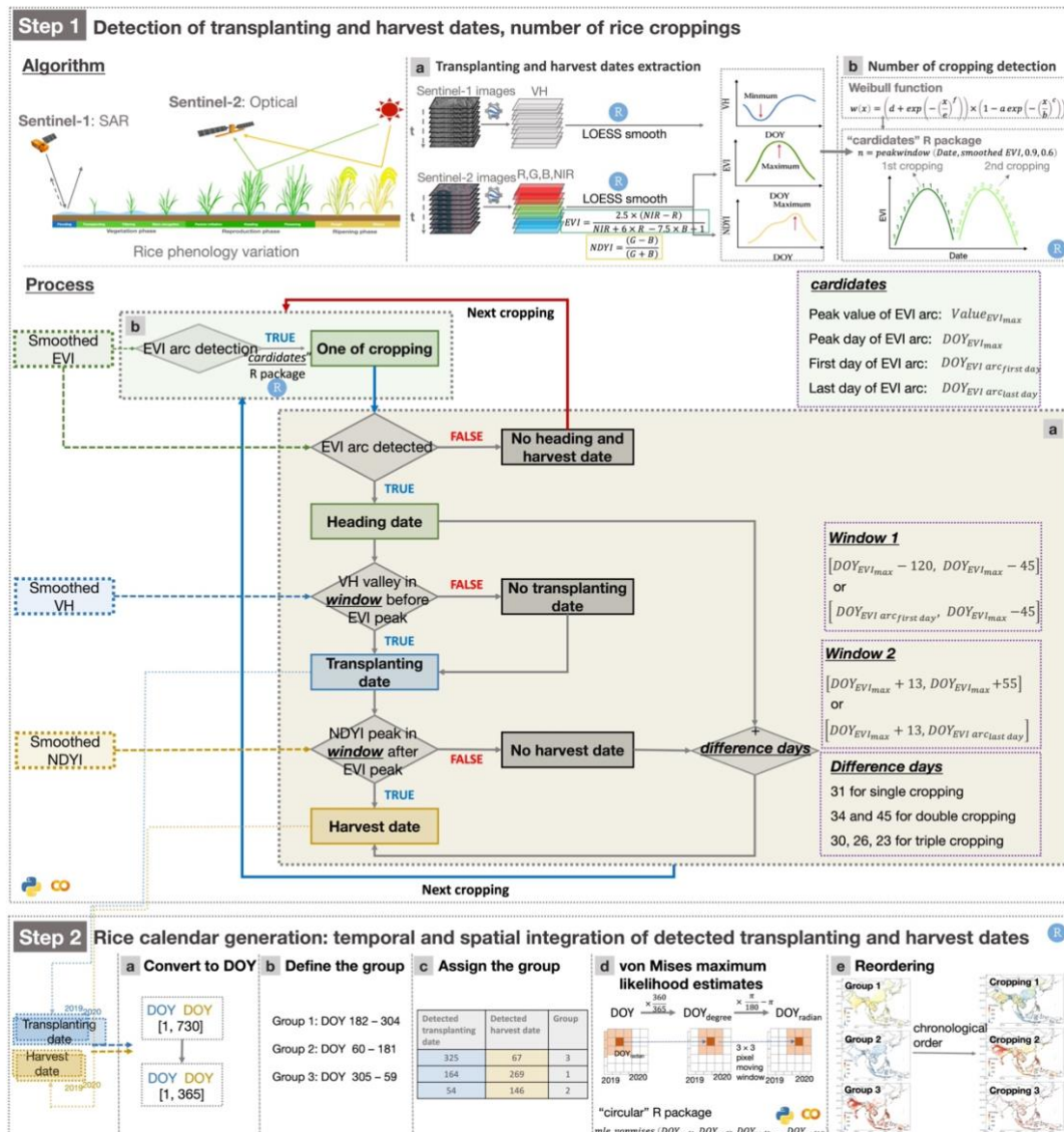


**Figure 2.** Workflow for gridded rice calendar mapping based on satellite images. Step 1 depicts the algorithm and process of transplanting and harvest dates extraction, along with the detection of number of rice croppings, as shown in the first box. In Step 2, the generation of the rice calendar is described, relying on the detected transplanting and harvest dates derived from Step 1, through the temporal and spatial integration of the detected phenological dates displayed in the second box (Page 9).

We have also revised the description of Step 1-1 and Step 1-2 in other contents as follows:

- **2.3.1.1 Algorithm (Step 1-1a) and process (Step 1-2b) for extraction of transplanting and harvest dates** (Line 200).
- **Additionally, rice harvest is characterized by irreversible leaf yellowing due to chlorophyll breakdown** (Zhang et al., 2021b) (Fig. 2 Step 1 Algorithm) (Lines 203-



209).

- The harvest date was detected using the NDYI's yellow signal, indicating the maximum yellowness at harvest date (Zhao et al., 2023) (Fig. 2 Step 1 Algorithm a) (Lines 217-221).
- The minimum VH and peak NDYI were detected within the time window (Fig. 2 Step 1 Process a), indicating that only the minimum VH and the maximum NDYI values within the time window, before and after the EVI peak, can be identified as the transplanting date and harvest date, respectively (Lines 223-225).
- If the peak NDYI could not be obtained from those time windows, peak NDYI was identified using the peak EVI date ( $DOY_{EVI_{max}}$ ) plus the corresponding difference days for each rice cropping, as referenced in Zhao et al. (2013) (Fig. 2 Step 1 Process a) (Lines 232-234).
- **2.3.1.2 Method (Step 1-1b) and process (Step 1-2a) for detecting the number of rice croppings** (Line 235).
- The six-parametric Weibull function,  $w(x) = \left( d + \exp\left(-\left(\frac{x}{a}\right)^f\right) \right) \times \left( 1 - \exp\left(-\left(\frac{x}{b}\right)^e\right) \right)$  (where  $a, b, c, d, e,$  and  $f$  are the free parameters to be fitted) (Rolinski et al., 2007), can be used to identify the number of rice croppings by depicting an arc with the shape of downward-opening patterns from the smoothed EVI time series (hereafter referred to as EVI arc) (Fig. 2 Step 1 Algorithm b) as shown follows (Lines 236-239).
- After application of the function (Eq. (74)), all available arcs of the smoothed EVI time series were then labelled, including the start (start day of detected EVI arc,  $DOY_{EVI\ arc\ first\ day}$ ), peak (peak day of detected EVI arc,  $DOY_{EVI_{max}}$ ), and end (end day of detected EVI arc,  $DOY_{EVI\ arc\ last\ day}$ ) of the arc, and the peak EVI value ( $Value_{EVI_{max}}$ ) (Fig. 2 Step 1 Process b) (Lines 252-254).
- ~~A~~ The rice feature-based phenology algorithm (Zhao et al., 2023) ~~was~~ applied to Sentinel-1 and Sentinel-2 images ~~to detect gridded rice transplanting and harvest dates~~ (Fig. 2 Step 1 Algorithm a). ~~This algorithm~~ successfully ~~extracted~~ rice

transplanting and harvest dates ~~from site to~~ at 0.5 grid-cell scale across monsoon Asia (Zhao et al., 2023) (Lines 468-470).

- The fitted Weibull function, implemented in the R package (Fig. 2 Step 1 Algorithm b), automatically detects the number of rice croppings based on the shape of the smoothed EVI time series, facilitating rapid and efficient rice calendar mapping (Lines 482-484).

***Anonymous referee #2:***

*In my opinion, the study is original and such datasets are needed; also, the approaches implementing Sentinel data in these tasks are important to develop. However, I have some major concerns regarding the manuscript which are described below.*

We greatly appreciate the valuable and constructive comments provided by the reviewer. In the following responses, we will address each comment point-by-point. The responses to the comments are presented in blue font, and changes to the manuscript are highlighted in red with a grey background.

*In the abstract, the authors state that other datasets are characterized by coarse resolution, while their dataset is, in fact, very coarse (0.5 degrees, approximately 55km). I suggest rephrasing or clarifying this statement. Also, why is the final calendar characterized by such low resolution when Sentinel data used in this study have a resolution of 10m?*

**Response:** We sincerely appreciate the reviewer's comments, and we acknowledge that the description of our rice calendar dataset may not be suitable. Although we want to convey the advantage of our proposed rice calendar – our spatial resolution surpasses that of existing large-scale rice calendars, which are typically produced at administrative scale ranging from country to sub-country levels – we have refrained from using the term “finer-resolution” in the Abstract section and “high spatial resolution” in the main text.

The revised contents are specifically as follows:

- This novel gridded rice calendar fills the gaps in half-degree rice calendars across major global rice production areas, facilitating research on rice phenology that is relevant to the climate change (Lines 27-29).
- The objective of this study was to develop a new gridded rice calendar that highlights the following features: (a) consistent detection using remote-sensing methods, (b) spatial resolution ( $0.5^\circ \times 0.5^\circ$ ), (c) large-scale coverage (monsoon Asia), and (d) ability to extract multiple rice croppings (Lines 110-112).
- The advantages of the above-mentioned algorithms (Fig 2 Step 1, Step 2) largely contribute to the production of a gridded rice calendar. ~~The proposed rice calendar fills the gaps in finer scale rice calendars with continental coverage using remote sensing methods.~~ The proposed rice calendar provides spatially explicit rice phenology with continental coverage through remote sensing methods. The major difference between the proposed rice calendar and the RICA rice calendar lies in the use of a feature-based algorithm with VH and NDYI, which allows the proposed rice calendar to theoretically estimate rice phenology more accurately. Zhao et al. (2023) demonstrated that VH can accurately capture the start of paddy water logging, and NDYI is a good indicator of rice maturity stage. The proposed rice calendar presents a highly patchy map of rice phenological information (Figs. 6 and 10a). The  $0.5^\circ$  resolution of the proposed rice calendar is finer than that of other rice calendars, including RiceAtlas, RICA at sub-national scale, and SAGE derived from sub-national data. This improvement greatly reduces the bias error caused by assigning averaged rice phenology to administrative units, as rice phenology can vary considerably within large administrative units (Franch et al., 2022). Furthermore, the proposed rice calendar displays the detailed distribution of rice paddy fields (Figs. 6 and 10a), in contrast to previous rice calendars that covered entire administrative areas, irrespective of the small proportion of rice cultivation (Figs. S6-S8 and 10b-d) (Lines 501-513).
- Given the absence of an updated global/continental-scale rice calendar that can explicitly depict spatial gridded transplanting date and harvest date information, and the number of rice croppings, this study developed a new gridded rice calendar

for monsoon Asia with **spatially explicit** detail of rice phenology using a new methodological framework based on Sentinel-1 and Sentinel-2 images (Lines 586-589).

The utilization of Sentinel images with a 10 m resolution contributes to improving the accuracy of rice calendar mapping because some rice paddy fields tend to be smaller than the 500 m resolution (Mishra et al., 2021). Sentinel satellites provide dense and detailed observations that can overcome the longer temporal frequency of Landsat images and the spatial resolution limitations of MODIS in mapping rice calendars. The objective of this work is to develop a large-scale rice calendar for monsoon Asia based on a more versatile methodology framework. The production of proposed half-grid rice calendar from Sentinel images is based on the following considerations: First, it greatly reduces the computation time and efficiently provides rice phenology information at a large scale. Second, the spatial resolution of proposed rice calendar surpasses that of existing large-scale rice calendars. Third, the 0.5° resolution fulfills the requirements for model simulation in estimating greenhouse gas emissions estimation.

*Furthermore, I have concerns regarding the accuracy assessment of the calendar. The dates of transplanting and harvesting are validated with the Rice Atlas, which has a national or subnational resolution, correct? It seems, therefore, inappropriate to validate the proposed calendar using such data.*

**Response:** We appreciate the reviewer's constructive comments. In our prior study (Zhao et al., 2023), we have already conducted rigorous validation of the rice phenology detection methods (feature-based algorithm) used in this calendar production at multiple spatial scales (sub-nation, 0.5° gridcell, and site scales) and across various

cropping systems (single, double, and triple croppings) in monsoon Asia. Results revealed biases in transplanting dates of 2, 0, and 4 days, while that in harvest dates of 2, -5, and -13 days at the sub-nation, 0.5° gridcell, and site scales, respectively (as demonstrated in Fig. 6, Fig. 7, Table 1, and Appendix A in Zhao et al. (2023)). This rigorous validation underscores the robustness of our proposed rice calendar (Zhao et al., 2023). Your point made us realize that we did not mention enough in the first draft about the results of past validation. So, we have added an explanation for this in the revised manuscript.

For the reason that we have conducted detailed validation in the previous study (Zhao et al., 2023), we have limited our dataset comparison in this paper to only those with broad datasets covering only the same geographic areas. Despite the coarse spatial resolution that does not correspond to our proposed rice calendar, RiceAtlas remains the only detailed global rice calendar to date (Laborte et al., 2017). Since its publication in 2017, RiceAtlas rice calendar has been cited 84 times (according to Web of Science). It stands as the widely accepted rice calendar extensively used in numerous research domains, including rice calendar validation (e.g., RICA rice calendar in Mishra et al. (2021) and model-based rice calendar in Iizumi et al. (2019)), mapping rice paddy field distribution (Han et al., 2021; Luintel et al., 2021), predicting rice production (Oort et al., 2017; Wu et al., 2023), and estimating methane emissions (Crippa et al., 2020; Ouyang et al., 2023). In fact, researchers regard RiceAtlas as the standard database for comparing rice phenology based on earth observation (Mishra et al., 2021). Therefore, we employed the RiceAtlas rice calendar to validate the transplanting and harvest dates. Our primary objective here is to compare the differences among similar large-scale rice calendar products. The absence of a half-grid rice calendar highlights the critical importance and necessity of our proposed rice calendar. We have included these points in the revised manuscript as follows:

- A feature-based algorithm, proposed for large-scale rice phenology detection (Zhao et al., 2023), excels in utilizing backscattering (VH) and vegetation indices

(Enhanced Vegetation Index (EVI) and Normalized Yellow Index (NDYI)) derived from Sentinel-1 & 2 to reflect features related to rice cultivation such as flooding, maximum leaf area, and most yellowness around transplanting, heading, and harvest date. Additionally, this algorithm has successfully tracked rice phenological dates in different cropping systems (single, double, and triple croppings) and at different spatial scales (sub-nation, 0.5° gridcell, and site scales) (Zhao et al., 2023) (Lines 94-99).

- These phenological characteristics of rice crops can be captured by a feature-based algorithm applied on smoothed VH, EVI, and NDYI time series data (Zhao et al., 2023). This algorithm's robustness has been confirmed at multiple spatial scales (sub-nation, 0.5° gridcell, and site scales) and cropping systems (single, double, and triple croppings) in monsoon Asia (Zhao et al., 2023). The transplanting date was determined by identifying the minimum VH intensity from the shortest plants above the water surface, where VH intensity gradually increase as they interact with the radar signal (Torres et al., 2012). The harvest date was detected using the NDYI's yellow signal, indicating the maximum yellowness at harvest date (Zhao et al., 2023) (Fig. 2 Step 1 Algorithm a) (Lines 210-221).

## References

- Zhao, X., Nishina, K., Akitsu, T.K., Jiang, L., Masutomi, Y., Nasahara, K.N.: Feature-based algorithm for large-scale rice phenology detection based on satellite images, *Agric. For. Meteorol.*, 329, 109283, <https://doi.org/10.1016/j.agrformet.2022.109283>, 2023.
- Laborte, A.G., Gutierrez, M.A., Balanza, J.G., Saito, K., Zwart, S.J., Boschetti, M., Murty, M.V.R., Villano, L., Aunario, J.K., Reinke, R., Koo, J., Hijmans, R.J., and Nelson, A.: RiceAtlas, a spatial database of global rice calendars and production, *Sci. Data*, 4, 170074, <https://doi.org/10.1038/sdata.2017.74>, 2017.
- Mishra, B., Busetto, L., Boschetti, M., Laborte, A., Nelson, A.: RICA: A rice crop calendar for Asia based on MODIS multi year data. *Int. J. Appl. Earth Obs. Geoinf.* 103, 102471, <https://doi.org/10.1016/j.jag.2021.102471>, 2021.

Iizumi, T., Kim, W., and Nishimori, M.: Modeling the global sowing and harvesting windows of major crops around the year 2000. *J. Adv. Model. Earth Syst.*, 11(1), 99-112, <https://doi.org/10.1029/2018MS001477>, 2019.

Han, J., Zhang, Z., Luo, Y., Cao, J., Zhang, L., Cheng, F., Zhuang, H., Zhang, J., Tao, F.: NESEA-Rice10: high-resolution annual paddy rice maps for Northeast and Southeast Asia from 2017 to 2019. *Earth Syst. Sci. Data*, 13, 5969-5986, <https://doi.org/10.5194/essd-13-5969-2021>, 2021.

Luintel, N., Ma, W., Ma, Y., Wang, B., Xu, J., Dawadi, B., Mishra, B.: Tracking the dynamics of paddy rice cultivation practice through MODIS time series and PhenoRice algorithm. *Agric. For. Meteorol.*, 307, 108538, <https://doi.org/10.1016/j.agrformet.2021.108538>, 2021.

van Oort, P.A.J. and Zwart, S.J.: Impacts of climate change on rice production in Africa and causes of simulated yield changes. *Glob. Change Biol.*, 24, 1029-1045, <https://doi.org/10.1111/gcb.13967>, 2018.

Wu, H., Zhang, J., Zhang, Z., Han, J., Cao, J., Zhang, L., Luo, Y., Mei, Q., Xu, J., Tao, F.: AsiaRiceYield4km: seasonal rice yield in Asia from 1995 to 2015. *Earth Syst. Sci. Data*, 15, 791-803, <https://doi.org/10.5194/essd-15-791-2023>, 2023.

Crippa, M., Solazzo, E., Huang, G., Guizzardi, D., Koffi, E., Muntean, M., Schieberle, C., Friedrich, R., Janssens-Maenhout, G.: High resolution temporal profiles in the emissions database for global atmospheric research. *Sci. Data*, 7, 121, <https://doi.org/10.1038/s41597-020-0462-2>, 2020.

Ouyang, Z., Jackson, R.B., McNicol, G., Fluet-Chouinard, E., Runkle, B.R.K., Papale, D., Knox, S.H., Cooley, S., Delwiche, K.B., Feron, S., Irvin, J.A., Malhotra, A., Muddasir, M., Sabbatini, S., Alberto, M.C.R., Cescatti, A., Chen, C., Dong, J., Fong, B.N., Guo, H., Hao, L., Iwata, H., Jia, Q., Ju, W., Kang, M., Li, H., Kim, J., Reba, M.L., Nayak, A.K., Roberti, D.R., Ryu, Y., Swain, C.K., Tsuang, B., Xiao, X., Yuan, W., Zhang, G., Zhang, Y., Paddy rice methane emissions across Monsoon Asia. *Remote Sens. Environ.*, 194, 348-365, 284, 113335, <https://doi.org/10.1016/j.rse.2022.113335>, 2023.

*In my opinion, the paper is too long, especially the discussion section, where some wordings and repetitions could be eliminated. The authors should reconsider the most crucial outcomes or applications of their approach and dataset. The limitations section, which is important, can be condensed into one or two paragraphs, for example. Some parts of the introduction can also be shortened. The methods are complex, resulting in a lengthy*



*chapter; however maybe the authors might consider moving certain sections to supplementary materials?*

**Response:** We appreciate the constructive feedback provided by the reviewer and have incorporated this suggestion into the revised manuscript. We have condensed the limitation section from six to two paragraphs but retained the main meaning. The revised content is as follows:

- One challenge is the limited experimental periods on which the calendar is based, specifically during 2019–2020. While it was facilitated by the GEE and Google Colaboratory, generating detailed detection for two years ( $127 \times 184 = 23,368$  grids  $\times 2$  years) still requires large computation power. Additionally, errors can arise from the spatial and temporal integration of transplanting and harvest dates. The grouping process, in particular, poses a risk of assigning single rice cropping seasons from two years into different groups, potentially overestimating the number of rice croppings. *Var* parameter, derived from the *mle.vonmises* function (Eqs. (429) and (441)), is prone to bias, requiring bias-corrected estimates when the sample size is less than 16 (Best and Fisher, 1981). To address these issues, a  $3 \times 3$  pixel window was used over two years to produce 18 values, highlighting the need to balance window size and sample size in spatio-temporal integration. The accuracy of reference rice calendars should also be considered, as they may rely on data from various sources and administrative scales (Laborte et al., 2017). Overlapping phenological dates between rice cropping seasons (Figs. S6–S8) can introduce further uncertainty. Furthermore, the complexity of multiple crop cropping systems can lead to an overestimation of rice croppings numbers. The growth of the other crop exhibits a similar pattern of a mono-peaked EVI time series and flood irrigation before sowing, similar to rice (Ahmad and Iram, 2023). Examples include the middle rice cropping system (rice with wheat, barley, or rapeseed cropping systems) in East and Central China (Chen et al., 2020) and the

rice–wheat cropping systems on the Indo-Gangetic Plain (Abrol, 1997; Dhanda et al., 2022) (Lines 516-530).

We have removed a sentence from Figure 11’s caption since it has been described in the revised manuscript on lines 401-403.

- **Figure 11.** Area of rice cropping of (a) the proposed rice calendar, (b) the RiceAtlas rice calendar, (c) the RICA rice calendar, and (d) the SAGE rice calendar. Blue, yellow, and red colours represent single, double, and triple rice cropping, respectively. Area calculation was based on the percentage of rice paddy field map (Fig. 1b) and area of each grid cell on the ellipsoidal earth (Fig. S8). (Lines 429-430).

We have removed the introductory description at the beginning of the “Advantages of the proposed rice calendar” section because this content has been discussed in other sections.

- ~~The aforementioned robustly supports the efficacy of the proposed rice calendar in depicting the detailed spatial variation of rice phenology across a large area. Thus, it can be considered a reliable gridded rice calendar for monsoon Asia. The use of remote sensing-based methods provides precise and timely monitoring of the phenological condition and development of rice crops. Furthermore, the combination of Sentinel 1 and Sentinel 2 imagery contributes to the spatial explicitness of the rice calendar because the Sentinel satellites are considered to open a new era of dense and detailed observations that could overcome the long temporal frequency of Landsat images and the spatial resolution limitations of MODIS in mapping rice calendars. Moreover, the Sentinel satellites were launched in 2014 and are scheduled to operate until 2030, thereby ensuring long-term continuous observation of rice phenology (Veloso et al., 2017).~~

We have shortened the sentence that discusses the algorithm’s advantages.

- A The rice feature-based phenology algorithm (Zhao et al., 2023) was applied to Sentinel-1 and Sentinel-2 images to detect gridded rice transplanting and harvest dates (Fig. 2 Step 1 Algorithm a). This algorithm successfully extracted rice transplanting and harvest dates from site to at 0.5 grid-cell scale across monsoon Asia (Zhao et al., 2023) (Lines 468-470).

We have removed the unsuitable description.

- The advantages of the above-mentioned algorithms (Fig 2 Step 1, Step 2) largely contribute to the production of a gridded rice calendar. The proposed rice calendar fills the gaps in finer scale rice calendars with continental coverage using remote sensing methods. The proposed rice calendar provides spatially explicit rice phenology with continental coverage through remote sensing methods (Lines 501-504).

Following your suggestions, we have shortened a part of the introduction section.

- However, many challenges hinder the production of accurate rice calendar using remote sensing approach. First, use of a coarse-moderate-resolution satellite sensor (e.g., AVHRR with approximately 5 km resolution and MODIS with 500 m resolution) or any single sensor (optical or synthetic aperture radar (SAR)) diminishes the accuracy of rice calendar mapping. The RICA rice calendar, produced using MODIS images, faces issues with rice paddy field sizes smaller than the 500 m sensor resolution (Mishra et al., 2021). Second, the rule-based algorithm currently in use for rice phenological date extraction depends on turning points or key nodes of vegetation indexes and backscattering (Xin et al., 2020), which are affected by the smoothing method and the parameters adopted. Additionally, existing algorithms like ChinaCropPhen1km for China (Luo et al., 2020) and EVI-related methods for Japan (Sakamoto et al., 2005) are limited to specific administrative areas. Some alternative algorithms like PhenoRice (Mishra et al., 2021) and LAI-related approaches (Zhang et al., 2022) aim to map rice

phenology at large areas but may ignore the fine heterogeneity within administrative units (Lines 56-76).

- The combination of optical and SAR sensors, utilizing the high spatial (10 m) and temporal (6 days for Sentinel-1, 5 days for Sentinel-2) resolution of Copernicus Sentinel images, benefits crop phenology monitoring by offering precise and timely information on phenological variations. A feature-based algorithm, proposed for large-scale rice phenology detection (Zhao et al., 2023), excels in utilizing backscattering (VH) and vegetation indices (Enhanced Vegetation Index (EVI) and Normalized Yellow Index (NDYI)) derived from Sentinel-1 & 2 to reflect features related to rice cultivation such as flooding, maximum leaf area, and most yellowness around transplanting, heading, and harvest date (Lines 87-97).

In response to the extensive Materials and methods section, we have shortened the section regarding “algorithm and process for extraction of transplanting and harvest dates” as follows:

- Flooding rice cultivation, common in Asia and accounting for over 12 % of the global cropland (FAOSTAT, 2020; Zhang et al., 2021a), presents a distinctive flooding signal that can be used for detection of rice transplanting date. Additionally, rice harvest is characterized by irreversible leaf yellowing due to chlorophyll breakdown (Zhang et al., 2021b) (Fig. 2 Step 1 Algorithm). These phenological characteristics of rice crops can be captured by a feature-based algorithm applied on smoothed VH, EVI, and NDYI time series data (Zhao et al., 2023). This algorithm’s robustness has been confirmed at multiple spatial scales (sub-nation, 0.5° gridcell, and site scales) and cropping systems (single, double, and triple croppings) in monsoon Asia (Zhao et al., 2023). The transplanting date was determined by identifying the minimum VH intensity from the shortest plants above the water surface, where VH intensity gradually increases as they interact with the radar signal (Torres et al., 2012). The harvest date was detected using the NDYI’s yellow signal, indicating the maximum yellowness at harvest date (Zhao

et al., 2023) (Fig. 2 Step 1 Algorithm a).

The minimum VH and peak NDYI were detected within the time window (Fig. 2 Step 1 Process a), indicating that only the minimum VH and the maximum NDYI values within the time window, before and after the EVI peak, can be identified as the transplanting date and harvest date, respectively. To identify the optimal window for detection of the transplanting and harvest dates, the time window for detection of the minimum VH and peak NDYI were used (Table S1). If the peak NDYI could not be obtained from those time windows, it was identified using the peak EVI date ( $DOY_{EVI_{max}}$ ) plus the corresponding difference days for each rice cropping, as referenced in Zhao et al. (2013) (Fig. 2 Step 1 Process a) (Lines 202-234).

Additionally, we have moved equations ( $R^2$ , Bias, MAE, RMSE) to Supplementary Text 1. The content of the optimal window for detecting transplanting and harvest dates was put into a table and moved to Supplementary Text 2. Please see the detailed response in two of the “other comments”. Moreover, we have made the following revisions:

- The reliability of this map is substantiated by its strong correlation with existing rice paddy field maps across diverse areas ( $R^2$  values ranging from 0.72 to 0.95) including China, North Korea, South Asia, and Southeast Asia, with  $R^2$  values ranging from 0.72 to 0.95, and its alignment with the area information obtained from FAOSTAT statistical data for each country (Zhang et al., 2020). Furthermore, this map aligns well with the area information obtained from FAOSTAT statistical data for each country (Zhang et al., 2020). Additionally, this map has been used to develop a feature-based algorithm for rice phenology detection (Zhao et al., 2023). (Lines 139-144).
- The RiceAtlas rice calendar, based on compilation of multiple census data sources, provides the start, peak, and end of the transplanting date and harvest date, and the number of rice croppings at national or sub-national scales globally. It is based on

~~compilation of multiple data sources that include census data, databases, publications, and reports~~ (Laborte et al., 2017) (Lines 168-171).

- The first step is extraction of transplanting and harvest dates and detection of the number of rice croppings, depicted in Fig. 2 Step 1-1 as the algorithm for phenological dates and number of rice croppings detection and in Fig. 2 Step 1-2 ~~as the process of phenological dates and number of rice croppings detection~~. The transplanting and harvest dates obtained in the first step (Step 1) require temporal and spatial integration for the generation of the rice calendar (Fig. 2 Step 2). ~~The following sections provide elaboration on the major procedures involved in each step.~~ (Lines 188-193).

*Finally, the GEE/Colab code is missing.*

**Response:** We greatly appreciate the reviewer’s comments and have added the Colab code in the revised manuscript. The added “Code availability” section is as follows:

- ~~The code for getting VH/EVI/NDYI time series data from Sentinel-1 and Sentinel-2 images, extracting the transplanting and harvest dates from smoothed VH/EVI/NDYI time series data, and spatial and temporal integration of detected transplanting and harvest dates can be found at <https://db-test.cger.nies.go.jp/DL/10.17595/20230728.001.html.en>~~ (Zhao and Nishina, 2023) (Lines 580-583).

*Other comments*

- *The link to dataset should be at the end of abstract also.*

**Response:** Thanks for your comments. We have added the link to dataset at the end of the Abstract:

➤ The developed gridded rice calendar in monsoon Asia is available at <https://www.nies.go.jp/doi/10.17595/20230728.001-e.html> (Zhao and Nishina, 2023) (Lines 29-30).

■ *In the abstract and in the whole manuscript I suggest changing units of area from  $5.3 \times 10^6$  to millions of kilometres, for example 5.3 mln of km.*

**Response:** Our apologies. The correct area is  $5.3 \times 10^5$  km<sup>2</sup> instead of  $5.3 \times 10^6$  km<sup>2</sup> according to the y-axis of Figure 11. Following your suggestion, we have converted the unit of area from  $5.3 \times 10^5$  km<sup>2</sup> to 0.53 million of km<sup>2</sup>. The revised contents are as follows:

➤ In total, the proposed rice calendar can detect single, double, and triple rice cropping with area of 0.53, 0.45, and 0.09 million of km<sup>2</sup>, respectively (Lines 25-27).

➤ The areas covered by single, double, and triple rice croppings in the proposed rice calendar area 0.53, 0.45, and 0.09 million of km<sup>2</sup>, respectively (Fig.11). The area covered by single rice cropping falls within the range of 0.24 million of km<sup>2</sup> (RiceAtlas rice calendar) to 0.65 million of km<sup>2</sup> (RICA rice calendar) (Fig.11) (Lines 416-418).

➤ Additionally, the area covered by triple rice cropping falls within the range of 0.05 million of km<sup>2</sup> (RICA rice calendar) to 0.4 million of km<sup>2</sup> (RiceAtlas rice calendar) (Lines 433-434).

■ *Line 106: rephrase to something like “The analysed area.... (Fig 1)”*

**Response:** Thanks for your suggestions. We have rephrased the description of study area. The revised sentence is as follows:

- **The analysed area is located in monsoon Asia, which covered the region of 10° S to 53.5° N, 61° E to 153° E (Lines 121-122).**
  
- *Figure 1 – so the study area includes all the countries shown in grey, with bold black borders – it is not fully clear from the figure, maybe add to legend. Also consider adding country names to the map.*

**Response:** We appreciate the reviewer's suggestion. We have added the legend of bold black borders to indicate the countries in the study area. At the same time, we have added the country names to the map. The revised Figure 1 is shown as follows:



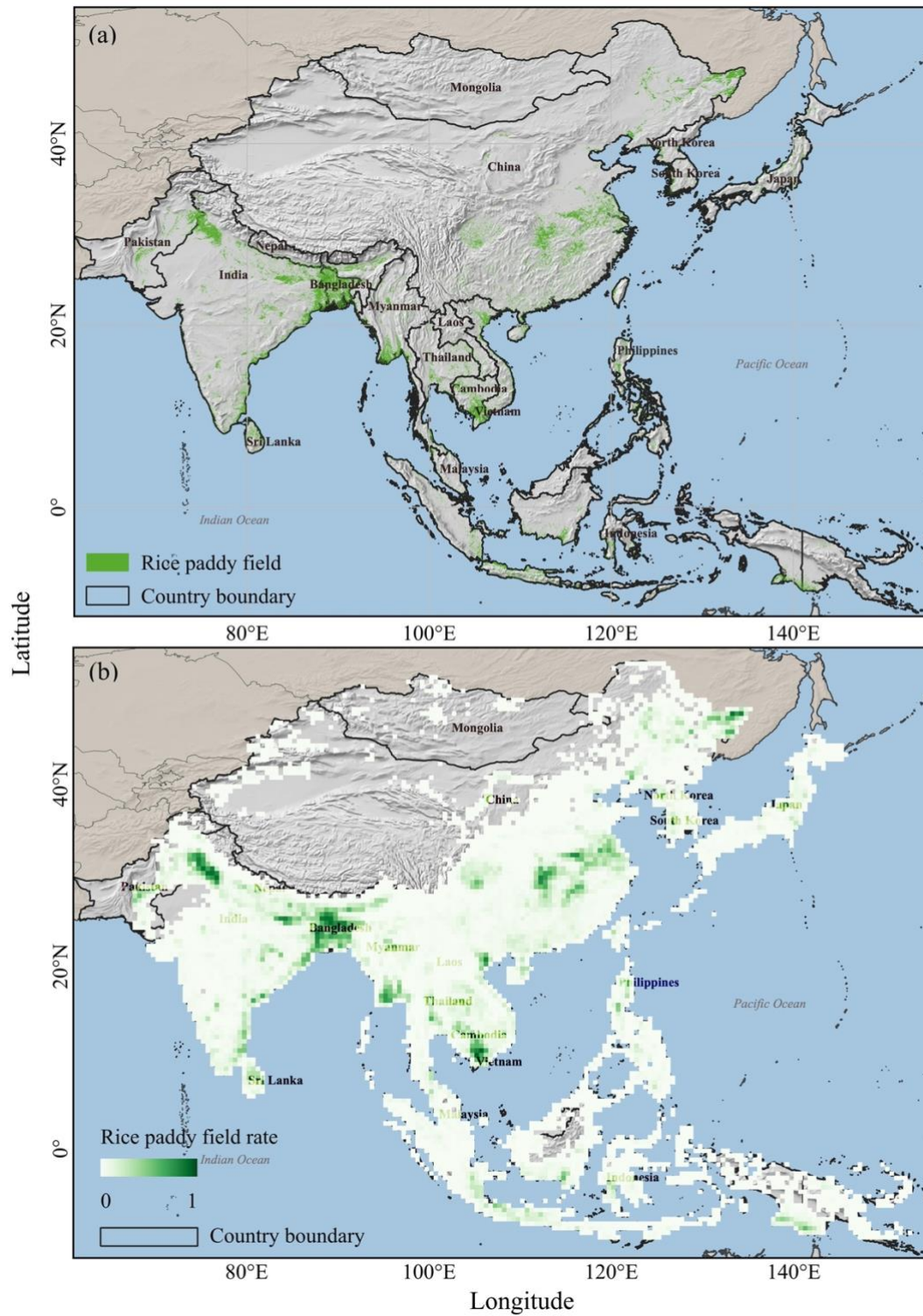
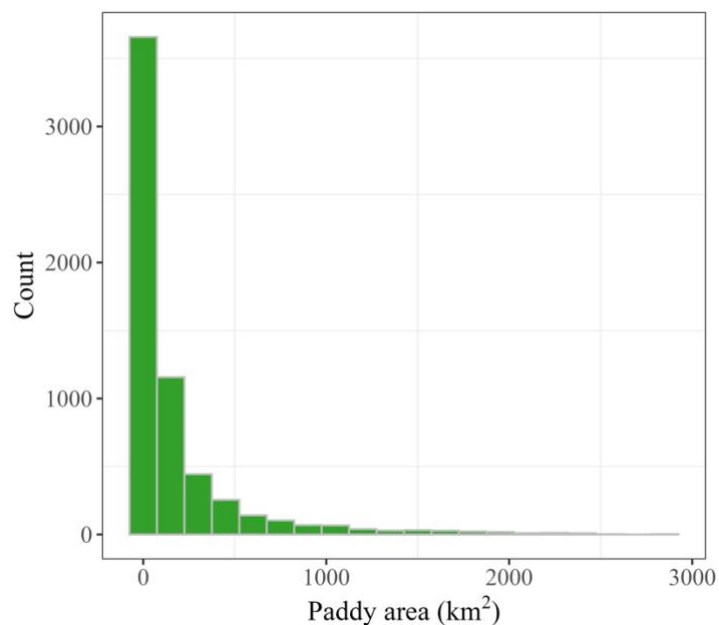


**Figure 1.** Location of the study area and distribution of rice paddy fields in monsoon Asia. Rice paddy field distribution map (a) was obtained from Zhang et al. (2020), which was proposed using MODIS images. Green areas indicate paddy fields, and bold black borders indicate the countries in this study area. Gridded rice paddy field map (b) shows the percentage of rice paddy field in 0.5° grids. Green gradient indicates variation in the percentage coverage of rice paddy fields (Page 5).

- *Line 130 – what is the average size of a paddy field in these regions, is 20 samples enough to represent it for such large grid?*

**Response:** Thank you for your question. The average size of paddy fields in a grid is 180 km<sup>2</sup>. This area was calculated by the percentage of rice paddy field in each grid (shown as Fig. 1b) multiplying the area of each grid cell on the ellipsoidal earth (Fig. S9). The distribution of the area of rice paddy fields in monsoon Asia is shown in the following figure, where 75% of grids have paddy rice filed areas of less than 180 km<sup>2</sup>. Thus, one sample could represent a rice paddy field of 9 km<sup>2</sup>, equivalent to 3,000 square meters. Although there is a slight gap between this and exact site-scale rice phenology, but it efficiently saves computation time and facilitates the implementation to obtain such broad-scale averaged rice phenology, based on the assumption that rice phenology is stable within a specific area.



Moreover, to demonstrate the rationale for sampling 20 rice paddy fields, we provide an example to address this issue, as shown in the following figure. In this example, 10,

20, 30, 40, and 50 rice paddy fields were randomly selected within four neighboring 0.5° grids. There is no difference in the extracted EVI peak days among the 20, 30, 40, and 50 sampled rice paddy fields for four grids. However, the 10 sampled rice paddy fields tend to yield different peak EVI days. We have included this figure as Fig. S2 in the Supplementary.

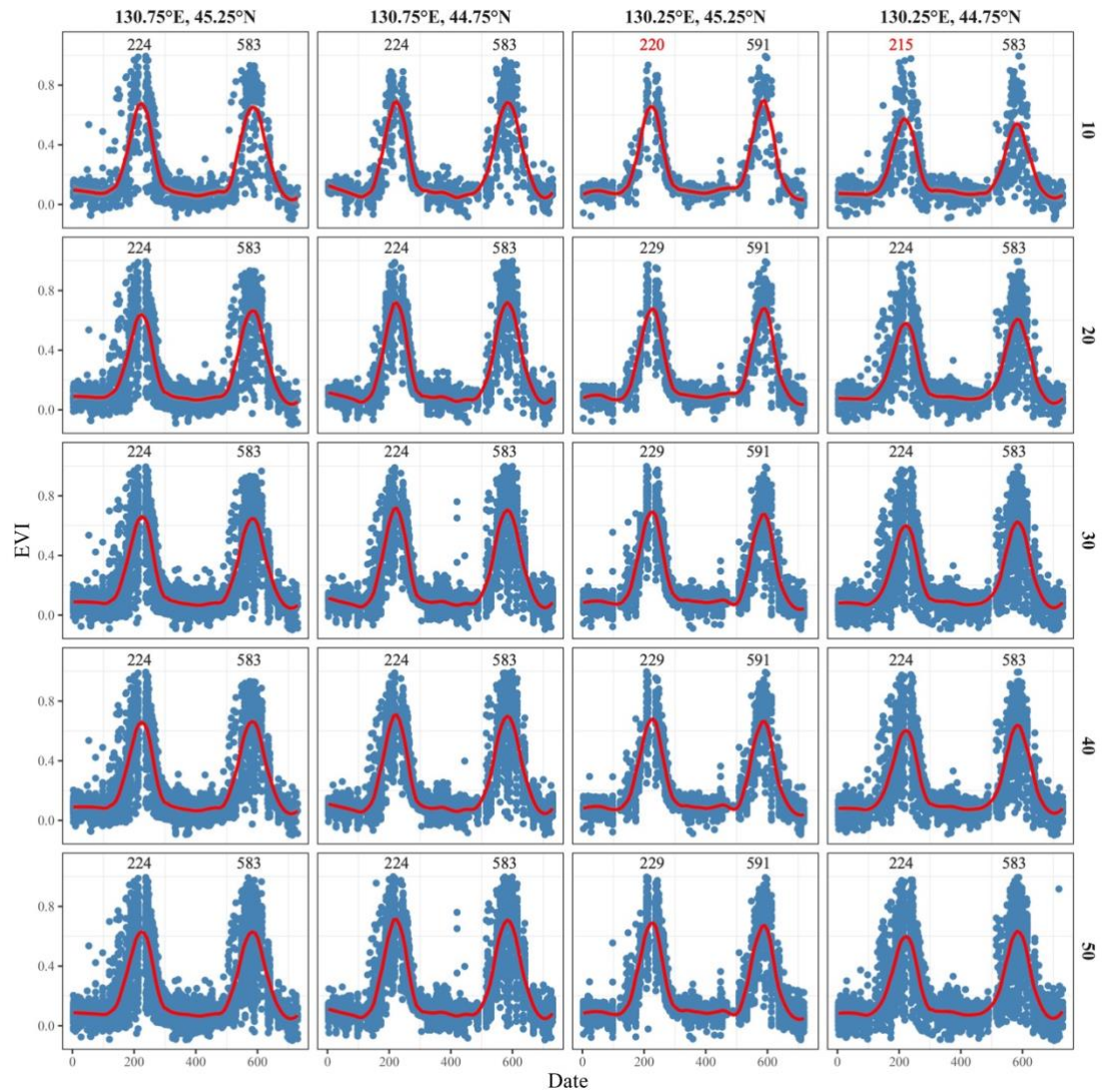


**Figure S2.** Example of the effect of sampling numbers in rice paddy fields (10, 20, 30, 40, and 50) for extracting phenological dates. X-axis denotes the days from 1 January 2019 to 31 December 2020, and Y-axis denotes the EVI values. The red line denotes the smoothed EVI values. The number in each panel denotes the extracted peak EVI days.

We have cited Fig. S2 in the “Rice paddy field distribution map and sampling method”

section to show how the sample size was determined, as follows:

- Additionally, this sampling size of 20 rice paddy fields is sufficiently enough that saves computation time and has no effect on averaged rice phenology detection (Fig. S2) (Lines 150-151).
  
- *Line 135 – the codes/notebooks should be included in the paper.*

**Response:** Thanks for your comments. We have added this code in the “Code availability” section as follows:

- The code for getting VH/EVI/NDYI time series data from Sentinel-1 and Sentinel-2 images, extracting the transplanting and harvest dates from smoothed VH/EVI/NDYI time series data, and spatial and temporal integration of detected transplanting and harvest dates can be found at <https://db-test.cger.nies.go.jp/DL/10.17595/20230728.001.html.en> (Zhao and Nishina, 2023) (Lines 580-583).
  
- *Line 160 – these are widely used metrics; I think their equations are redundant*

**Response:** We agree with you that these equations are widely used. Consequently, we have moved them to Supplementary Text 1. The revised content in the Manuscript is as follows:

- The RiceAtlas rice calendar, with its detailed phenological date range, was used to assess the performance of the proposed rice calendar in determining transplanting date and harvest date, evaluating it based on the performance of the

proposed rice calendar in determining transplanting and harvest dates was assessed using the coefficient of determination ( $R^2$ ), bias error (Bias), Mean Absolute Error (MAE), and Root Mean Square Error (RMSE) (Supplementary Text 1) which were calculated as follows: (Lines 175-186).

$$R^2 = 1 - \frac{(\sum_{i=1}^n (y_i - \bar{y})(s_i - \bar{s}))^2}{\sum_{i=1}^n (y_i - \bar{y})^2 - \sum_{i=1}^n (s_i - \bar{s})^2} \quad (3)$$

$$Bias = \frac{1}{n} \sum_{i=1}^n (y_i - s_i) \quad (4)$$

$$MAE = \frac{1}{n} \sum_{i=1}^n |y_i - s_i| \quad (5)$$

$$RMSE = \sqrt{\frac{1}{n} \sum_{i=1}^n (y_i - s_i)^2} \quad (6)$$

where  $y_i$  and  $\bar{y}$  are the phenological dates from the proposed rice calendar for sample grid ( $i$ ) and the corresponding mean value, respectively,  $s_i$  and  $\bar{s}$  are the phenological dates from the reference rice calendar for sample grid ( $i$ ) and the corresponding mean value, respectively, and  $n$  represents the number of sampled phenological dates.

The revised content in the Supplementary Text 1 is as follows:

➤ **1. Performance of the proposed rice calendar**

The performance of the proposed rice calendar in determining the transplanting and harvest dates was assessed using the coefficient of determination ( $R^2$ ), bias error (Bias), Mean Absolute Error (MAE), and Root Mean Square Error (RMSE) which were calculated as follows:

$$R^2 = 1 - \frac{(\sum_{i=1}^n (y_i - \bar{y})(s_i - \bar{s}))^2}{\sum_{i=1}^n (y_i - \bar{y})^2 - \sum_{i=1}^n (s_i - \bar{s})^2} \quad (1)$$

$$Bias = \frac{1}{n} \sum_{i=1}^n (y_i - s_i) \quad (2)$$

$$MAE = \frac{1}{n} \sum_{i=1}^n |y_i - s_i| \quad (3)$$

$$RMSE = \sqrt{\frac{1}{n} \sum_{i=1}^n (y_i - s_i)^2} \quad (4)$$

where  $y_i$  and  $\bar{y}$  are the phenological dates from the proposed rice calendar for sample grid ( $i$ ) and the corresponding mean value, respectively,  $s_i$  and  $\bar{s}$  are the phenological dates from the reference rice calendar for sample grid ( $i$ ) and the corresponding mean value, respectively, and  $n$  represents the number of sampled phenological dates.

- *Lines 197-205 – this is very complex and somehow hard to follow. Maybe it can be put into a table and moved it to supplementary materials. Also, why such dates were used?*

**Response:** We greatly appreciate the reviewer’s valuable suggestions. Following your advice, we have organized this content into a table and relocated it to the Supplementary Text 2. In this study, we used these days to identify the optimal windows for detecting transplanting and harvest dates, specifically, the minimum VH and peak NDYI were extracted from the ranges of these days. This implementation aims to ensure the extraction of the minimum VH and peak NDYI, as any bias in peak or valley could lead to errors in determining transplanting or harvest dates, especially in the case of double and triple rice croppings. The revised content in the manuscript is as follows:

- ~~To identify the optimal window for detection of the transplanting and harvest dates, the time window for detection of the minimum VH and peak NDYI were used (Table S1). To identify the optimal time window for detection of the transplanting and harvest dates, the time window for detection of the minimum VH was set from 120 days before the date of peak EVI ( $DOY_{EVI_{max}}$ ) to 45 days before the date of peak EVI, i.e.,  $[DOY_{EVI_{max}} - 120, DOY_{EVI_{max}} - 45]$  or from the first day of EVI are ( $DOY_{EVI_{arc\_first\_day}}$ ) to 45 days before the date of peak EVI, i.e.,  $[DOY_{EVI_{arc\_first\_day}}, DOY_{EVI_{max}} - 45]$ . The time window for detection of the peak NDYI was set from 13 days after the peak EVI date to 55 days after the date of~~

peak EVI, i.e.,  $[DOY_{EVI_{max}} + 13, DOY_{EVI_{max}} + 55]$  or from 13 days after the peak EVI date to the last day of the EVI arc ( $DOY_{EVI_{arc_{last\ day}}}$ ), i.e.,  $[DOY_{EVI_{max}} + 13, DOY_{EVI_{arc_{last\ day}}}]$  (Lines 225-232).

The revised content in the Supplementary Text 2 is as follows:

➤ **2. Optimal time window for transplanting and harvest dates detection**

To identify the optimal time window for detection of the transplanting and harvest dates, the time window for detection of the minimum VH was set from 120 days before the date of peak EVI to 45 days before the date of peak EVI ( $DOY_{EVI_{max}}$ ), or from the first day of EVI arc ( $DOY_{EVI_{arc_{first\ day}}}$ ) to 45 days before the date of peak EVI. The time window for detection of the peak NDYI was set from 13 days after the peak EVI date to 55 days after the date of peak EVI, or from 13 days after the peak EVI date to the last day of the EVI arc ( $DOY_{EVI_{arc_{last\ day}}}$ ). It can be shown as follow table.

**Table S1.** Optimal time window for transplanting and harvest dates detection

Time window	Transplanting date	Harvest date
1	$[DOY_{EVI_{max}} - 120, DOY_{EVI_{max}} - 45]$	$[DOY_{EVI_{max}} + 13, DOY_{EVI_{max}} + 55]$
2	$[DOY_{EVI_{arc_{first\ day}}}, DOY_{EVI_{max}} - 45]$	$[DOY_{EVI_{max}} + 13, DOY_{EVI_{arc_{last\ day}}}]$

- *Line 200 – what is EVI arc?*

**Response:** The EVI arc denotes the arc with the shape of downward-opening patterns from the smoothed EVI time series. We have addressed it on the revised content as follows:

➤ The six-parametric Weibull function,  $w(x) = \left(d + \exp\left(-\left(\frac{x}{e}\right)^f\right)\right) \times \left(1 - a \exp\left(-\left(\frac{x}{b}\right)^c\right)\right)$  (where  $a, b, c, d, e,$  and  $f$  are the free parameters to be fitted) (Rolinski et al., 2007), can be used to identify the number of rice croppings by depicting an arc with the shape of downward-opening patterns from the smoothed EVI time series (hereafter referred to as EVI arc) (Fig. 2 Step 1 Algorithm b), as shown follows: (Lines 236-239).

■ Line 207 – that part as the equation format

**Response:** Yes, that part should be shown as the equation format. We have revised this part as follows:

➤ The six-parametric Weibull function,  $w(x) = \left(d + \exp\left(-\left(\frac{x}{e}\right)^f\right)\right) \times \left(1 - a \exp\left(-\left(\frac{x}{b}\right)^c\right)\right)$  (where  $a, b, c, d, e,$  and  $f$  are the free parameters to be fitted) (Rolinski et al., 2007), can be used to identify the number of rice croppings by depicting an arc with the shape of downward-opening patterns from the smoothed EVI time series (hereafter referred to as EVI arc) (Fig. 2 Step 1 Algorithm b), as shown follows:

$$w(x) = \left(d + \exp\left(-\left(\frac{x}{e}\right)^f\right)\right) \times \left(1 - a \exp\left(-\left(\frac{x}{b}\right)^c\right)\right) \quad (3)$$

{where  $a, b, c, d, e,$  and  $f$  are the free parameters to be fitted} (Rolinski et al., 2007) (Lines 236-241).

As the equations of coefficient of determination ( $R^2$ ) (Eq. (3)), bias error (Bias) (Eq. (4)), Mean Absolute Error (MAE) (Eq. (5)), and Root Mean Square Error (RMSE) (Eq.



(6)) have been removed, the six-parametric Weibull function has thus been designated as Eq. (3). Consequently, and the equation numbering has been adjusted from 7 to 16 to 4 to 13. Correspondingly, the numbering of equations in the text has been revised as follows:

- After application of the function (Eq. (74)), all available arcs of the smoothed EVI time series were then labelled, including the start (start day of detected EVI arc,  $DOY_{EVI\ arc\ first\ day}$ ), peak (peak day of detected EVI arc,  $DOY_{EVI_{max}}$ ), and end (end day of detected EVI arc,  $DOY_{EVI\ arc\ last\ day}$ ) of the arc, and the peak EVI value ( $Value_{EVI_{max}}$ ) (Fig. 2 Step 1 Process b) (Lines 252-254).
  - where  $\mu$  is the mean direction of the distribution, and  $\kappa$  is a non-negative numeric value representing a concentration parameter of the distribution;  $\mu$  and  $\kappa$  are correspond to  $\mu$  and  $\kappa$  in Eq. (85), respectively (Lines 303-304).
  - The circular data  $x$  in Eqs. (85) and (96) denote the phenological date shown in DOY format (Line 306).
  - The parameters  $DOY_{integrated}$  and  $Var$  were derived from the mle.vonmises function (Eq. (129)), representing the value and variance of the phenological dates ( $DOY_{rad}$ ), respectively (Lines 319-320).
  - $Var$  parameter, derived from the mle.vonmises function (Eqs. (129) and (1411)), is prone to bias, requiring bias-corrected estimates when the sample size is less than 16 (Best and Fisher, 1981) (Lines 520-522).
- Line 210 – From R: “To cite package 'carddates' in publications use: Rolinski, S., Horn, H., Petzoldt, T., Paul, L. (2007). Identification of cardinal dates in phytoplankton time series to enable the analysis of long-term trends. *Oecologia* 153, 997--1008. doi:10.1007/s00442-007-0783-2”

**Response:** Thanks for your suggestion. We have cited the package “carddates” using the following reference:

Rolinski, S., Horn, H., Petzoldt, T., and Paul, L.: Identifying cardinal dates in phytoplankton time series to enable the analysis of long-term trends. *Oecologia* 153, 997-1008. <https://doi.org/10.1007/s00442-007-0783-2>, 2007.

Consequently, the revised contents are as follows:

- This fitted Weibull function can be implemented using the peakwindow function in the carddates” package of R (Petzoldt et al., 2023; Rolinski et al., 2018; R Core Team, 2013) (<https://cran.r-project.org/web/packages/carddates/index.html>) (Rolinski et al., 2007) (Fig. S3a; Fig. 3) (Lines 242-244).

Correspondingly, the unreferenced sources have been removed from the References section:

- ~~Petzoldt, T., Sachse, R., and Rolinski, S.: Quickstart manual for package carddates, <https://cran.r-project.org/web/packages/carddates/vignettes/vignette.pdf>, last access: 2 May 2023.~~
- ~~R Core Team: R: A language and environment for statistical computing, 2013.~~
- ~~Rolinski, S., Sachse, R., and Petzoldt, T.: carddates: Identification of cardinal dates in ecological time series, R package version 0.4.8, <http://carddates.r-forge.r-project.org>, 2018.~~

- *Figure 3 description: there is no grey area in the charts*

**Response:** We apology for the error. We have revised the caption of Figure 3 as follows:

- **Figure 3.** Smoothed EVI time series and subsequent identification of the number of rice croppings at adjacent grids (32.25°N, 130.25°E, and 32.75°N, 130.25°E) across two years. Left column shows the smoothed EVI time series using the

LOESS method. Black points and green lines indicate the EVI value at specific dates and the smoothed EVI time series, respectively. Green area indicates the 95 % confidence interval around the smoothed EVI time series. Right column displays the number of rice croppings detected using the fitted Weibull function implemented via the “carditates” package in R. Blue, yellow, red, and black lines correspond to the detected first, second, third, and fourth arcs of the smoothed EVI time series (Lines 261-266).

- *Line 265 – cite the ‘circular’ package properly*

**Response:** Thanks. We have cited the “circular” package as follows:

- The availability of the “circular” R package (<https://rdrr.io/rforge/circular/man/circular-package.html>) (Agostinelli and Lund, 2023) is convenient for analysis of circular data (Lines 299-300).

This new reference has been added to the “References” section:

- Agostinelli, C., and Lund, U.: R package “circular”: Circular Statistics (version 0.5–0). <https://CRAN.R-project.org/package=circular>, 2023 (Lines 611-612).
- *The figures 4-7 – parts of the figures’ captions are redundant as they include the information already provided in the figure (e.g., what is in upper, middle lower panels etc.)*

**Response:** We've fully accepted your suggestions and removed the redundant parts in the captions from Figure 4 to Figure 7 as follows:

- **Figure 4.** Transplanting date and harvest date for the three groups. ~~Upper, middle, and lower panels of the left column show the transplanting date for Group 1, Group 2, and Group 3, respectively. Upper, middle, and lower panels of the right column show the harvest date for Group 1, Group 2, and Group 3, respectively.~~ Colour gradient from blue to red in the legend denotes the respective transplanting and harvest dates (Lines 347-350).
- **Figure 5.** Variance in transplanting date and harvest date for the three groups. ~~Upper, middle, and lower panels of the left column show the variance in transplanting date for Group 1, Group 2, and Group 3, respectively. Upper, middle, and lower panels of the right column show the variance in harvest date for Group 1, Group 2, and Group 3, respectively.~~ Colour gradient from blue to red in the legend denotes the respective variance in transplanting and harvest dates (Lines 352-355).
- **Figure 6.** Transplanting date and harvest date for three rice croppings. ~~Upper, middle, and lower panels of the left column show the transplanting date for Cropping 1, Cropping 2, and Cropping 3, respectively. Upper, middle, and lower panels of the right column show the harvest date for Cropping 1, Cropping 2, and Cropping 3, respectively.~~ Colour gradient from blue to red in the legend denotes the respective transplanting and harvest dates (Lines 366-369).
- **Figure 7.** Variance in transplanting date and harvest date for three rice croppings. ~~Upper, middle, and lower panels of the left column show the variance in transplanting date for Cropping 1, Cropping 2, and Cropping 3, respectively. Upper, middle, and lower panels of the right column show the variance in harvest date for Cropping 1, Cropping 2, and Cropping 3, respectively.~~ Colour gradient from blue to red in the legend denotes the respective variance in transplanting and harvest dates (Lines 372-375).

At the same time, we have removed the redundant parts in the captions from Figure S5 to Figure S7 in the Supplementary material as follows:

- **Figure S6.** Transplanting and harvest dates from the RiceAtlas calendar. ~~Upper, middle, and lower panels of the left column show the transplanting date for Cropping 1, Cropping 2, and Cropping 3, respectively. Upper, middle, and lower panels of the right column show the harvest date for Cropping 1, Cropping 2, and Cropping 3, respectively.~~ Colour gradient from blue to red in the legend denotes the respective transplanting and harvest dates.
- **Figure S6.** Transplanting and harvest dates from the RICA calendar. ~~Upper, middle, and lower panels of the left column show the transplanting date for Cropping 1, Cropping 2, and Cropping 3, respectively. Upper, middle, and lower panels of the right column show the harvest date for Cropping 1, Cropping 2, and Cropping 3, respectively.~~ Colour gradient from blue to red in the legend denotes the respective transplanting and harvest dates.
- **Figure S8.** Transplanting and harvest dates from the SAGE calendar. ~~Upper, middle, and lower panels of the left column show the transplanting date for Cropping 1, Cropping 2, and Cropping 3, respectively. Upper, middle, and lower panels of the right column show the harvest date for Cropping 1, Cropping 2, and Cropping 3, respectively.~~ Colour gradient from blue to red in the legend denotes the respective transplanting and harvest dates.

- *Lines 303-305 – maybe add median dates to the figures as well*

**Response:** We sincerely appreciate the reviewer’s comments. The median date for each cropping here was statistically calculated from all grids across monsoon Asia. In other words, it was derived from the results presented in Fig. 4 and Fig. 6. The phenological date in each grid of Fig. 4 is obtained from the mean of the 18 grids ( $3 \times 3$  grids  $\times 2$

years) using the von Mises maximum likelihood estimates methods shown in Step 2. So we keep it as it.

- *Figure 9 caption – there is no grey dotted line*

**Response:** We apologize for the error. The “Grey dotted line” should be replaced with the “Black solid line”. The revised caption of Figure 9 is as follows:

- **Figure 9.** Comparison of transplanting date and harvest date for single rice cropping between the proposed rice calendar and the RiceAtlas rice calendar. Blue and orange represent the transplanting date and harvest date, respectively; vertical lines denote the range of the transplanting and harvest dates for the proposed rice calendar; horizontal lines denote the range of the transplanting and harvest dates of the RiceAtlas rice calendar; dots denote the peak of the transplanting or harvest dates. Black dots denote the detected phenological day that falls within the transplanting or harvest ranges from the RiceAtlas rice calendar. Red and black solid lines represent the 1:1 line and regression, respectively (Lines 396-401).